Proceedings World Geothermal Congress 2020+1
Reykjavik, Iceland, April - October 2021

Improvement Research of Condensing Equipment in Organic Rankine Cycle Power Generation Systems

Jiaqi Zhang, Wei Zhang, Xinli Lu, Dawei Guo

Key Laboratory of Efficient Utilization of Low and Medium Grade Energy, MOE, Tianjin University, China

zhang_wei@tju.edu.cn

Keywords: organic Rankine cycle, closed wet cooling tower, pressure drop, net power generation, net generation efficiency.

ABSTRACT

Dry hot rock power generation is an important part of geothermal energy application, and the condenser has become an important part of the system because it can provide a lower outlet back pressure for the steam turbine, and improve the power generation of the system. Engineering Equation Solver is applied to assess the performance of cooling towers for organic Rankine cycle power generation systems. In the present study, two models with different cooling towers are considered: In the first model, the predicted performance of the opening cooling tower for organic Rankine cycle systems is studied and compared with the experimental measurement for a 500 kW system. In the second model, because of the high mass flow of the cooling water and high energy consumption of the cooling water pump for the opening cooling tower, the predicted performance of the closed wet cooling tower to replace the opening cooling tower for organic Rankine cycle systems is studied. The models are capable of predicting the variation of evaporation and condensation temperatures, the pressure loss of heat exchangers. R123, R227ea, R245fa, R600 and R600a are tested as working fluids. The results show that the second model reduces the energy consumption of the cooling water pump, and it also improves the net power generation and net generation efficiency for using R227ea, R600, R600a. However, with the increase of the closed wet cooling tower pressure loss, both the net power generation and net generation efficiency decrease. Therefore, different working fluids are suitable for different pressure loss.

1. INTRODUCTION

An organic Rankine cycle (ORC) power generation system has been extensively studied because it can effectively utilize medium and low temperature heat sources. Hasan Koten (2018) carried out a detailed study of the ORC system and a variety of working fluids, and concluded that its power generation efficiency is between 10-20%. As an important part of the ORC system, the condenser can provide a lower outlet back pressure for the steam turbine to improve the power generation of the system. So many scholars have done a lot of research on the condenser. Abdullah (2013) established a 3D computational fluid dynamics (CFD) model of the spray water and validated against experimental measurements obtained from a wind tunnel test. Yang (2012, 2013) established a mathematical model based on four 660 MW dry cooling towers, and studied the effects of the air velocity, pressure and temperature on the performance of the cooling tower under different wind speeds and directions. Kamel (2010) established a dry cooling tower model treating the heat exchanger as porous medium, and studied the turbulent free convection flowing through the heat exchanger tube bundle and cooling tower, finally they put forward the scaling law for dry cooling tower. There are also many detailed researches studied on dry cooling towers by Preez (1993,1995) and AL-Waked R (2004).

Compared to dry cooling towers, wet cooling towers offer a better performance. Numerous researches studied a detailed description on the application of wet cooling towers. Jiang (2013) designed a cross-flow CWCT unit, and they found the heat and mass transfer coefficients and cooling efficiency were remarkably affected by the temperature of the process water and the flow rates of the air, the spray water and the process water. Various researches studied the effect of air condition on the performance of the cooling tower by Kloppers (2005), Heidarinejad G (2009) and Papaefthimiou V D (2011). Mani (2008) found that the effect of web bulb temperature of the inflow air on the performance of wet cooling towers is more significant than the temperature of inflow water. Ebrahim (2010) studied the effect of the dry bulb temperature of inflow air on the performance of the crossflow wet cooling tower. Other studies dealt with the exergy processes occurring in the CWCT by the simulation and experiment Wang L (2011). Muangnoi (2007) established a mathematical model based on the height of cooling tower and exergy analysis, and the results showed that the exergy loss attained the maximum at the bottom of cooling towers and the minimum at the top of it. A large number of researches studied the efficiency and economy, pressure loss and application of the CWCT. Khan J U R (2004) and Saidi M H (2011). Gan G (2001) established a CFD model of the closed wet cooling tower. By comparing with the experimental measurement, they concluded that CFD can be used to assess the effect of the flow interference on the fluid distribution and pressure loss of single- and multi-phase flow over the heat exchanger. Walraven D (2015) made a comprehensive analysis of the cooling tower of the ORC system, they found that compared to the natural ventilation cooling tower, the mechanical ventilation cooling tower has a better economic performance. And the dry bulb temperature of air plays an important role on the cooling effect.

Above all, it can be found that compared to the opening cooling tower (OCT), the CWCT has a better cooling performance. Therefore, this paper implements the CWCT instead of the traditional condensing equipment (composed of the shell-and-tube condenser and the OCT), as shown in Figure 1 and Figure 2. The work of this paper mainly focuses on the following aspects: 1. The model of the ORC system is established and compared with the experimental measurement; 2. The model of using CWCT as the condensing equipment is established; 3. Comparing the two models, the energy consumption of the cooling water pump, the net power generation and net generation efficiency are studied and analyzed.

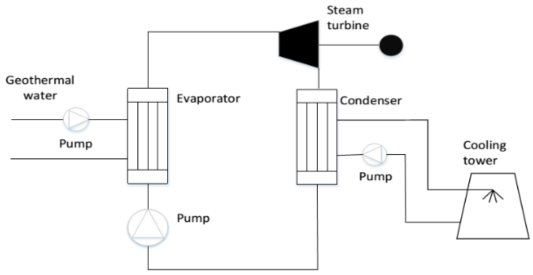

Figure 1: Schematic diagram of the OCT-ORC power generation system.

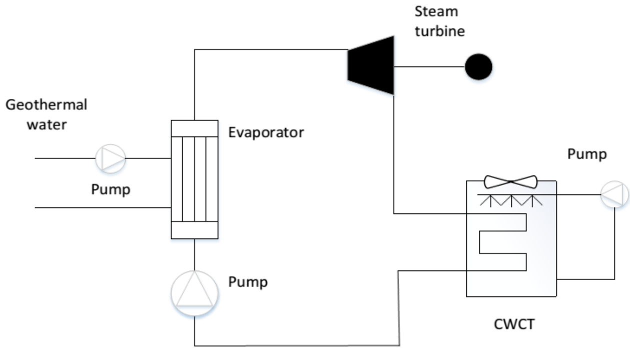

Figure 2: Schematic diagram of the CWCT-ORC power generation system.

2. OCT-ORC POWER GENERATION SYSTEM MODELS

2.1 OCT-ORC Systems

Figure 3 shows the *T-S* diagram of the ORC system. The working fluid absorbs heat in the evaporator (point 1) and becomes high pressure vapor. Then, the high pressure vapor flows into the steam turbine and becomes the low pressure steam (point 2,2s). The low pressure steam is condensed in the condenser and becomes the saturated liquid (point 4). Finally, it is pumped to the evaporator, forming a circulation. In the ideal state, the steam turbine power generation process is isentropic process (1-2s), but in reality, the process 1-2 depends on the generation efficiency.

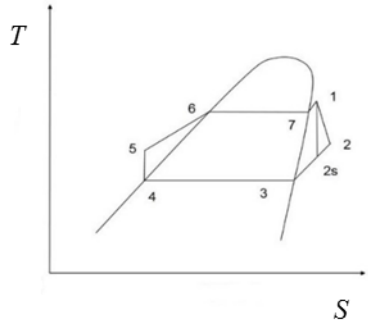

Figure 3: *T-S* diagram of the ORC system.

Among them, the model of the ORC power generation system using OCT as the condensation equipment (OCT-ORC) is established. The model selects R123，R227ea，R245fa，R600 and R600a as working fluids. The model of the ORC system is established by Engineering Equation Solver (EES), with the main equations of the model as follows:

The heat of the working fluids observed in evaporator is given by

$$m_{\mathrm{orc}} \cdot (h_1 - h_5) = m_{\mathrm{hw}} \cdot \left(h_{\mathrm{hw,in}} - h_{\mathrm{hw,out}}\right) = Q \tag{1}$$

The power generation of the steam turbine is computed from

$$W = (h_1 - h_{2s}) \cdot \eta_{\mathrm{is}} \tag{2}$$

$$W_{\mathrm{output}} = W \cdot \eta_{\mathrm{m}} \cdot \eta_{\mathrm{e}} \tag{3}$$

The load of the condensation equipment is defined as

$$m_{\mathrm{orc}} \cdot (h_2 - h_4) = c \cdot m_{\mathrm{cw}} \cdot (T_{\mathrm{cw,in}} - T_{\mathrm{cw,out}}) \tag{4}$$

Energy consumption of the working fluid pump is written as

$$W_{\mathrm{orc,p}} = m_{\mathrm{orc}} \cdot (h_5 - h_4)/\eta_{\mathrm{orc,p}} \tag{5}$$

Energy consumption of the cooling water pump is defined as

$$W_{\mathrm{cw,p}} = m_{\mathrm{cw}} \cdot g \cdot H/(\eta_{\mathrm{cw,p}} \cdot 1000) \tag{6}$$

The net power generation and net generation efficiency of the system are written as

$$W_{\mathrm{net}} = \mathrm{W}_{out} - W_{\mathrm{orc,p}} - W_{\mathrm{cw,p}} - W_{\mathrm{fan}} \tag{7}$$

$$\eta = W_{\mathrm{net}}/Q \tag{8}$$

Before calculating the model, some assumptions are made about the model:

(1) Theoretically, the cooling capacity of the cooling tower is 6-10 °C, but according to the local environmental factors of the experiment, the capacity of setting the cooling tower is 3 °C.

(2) Suppose that the outlet state of refrigerant condenser is saturated liquid.

In addition, some basic parameters of each component in the system are also set up, as shown in Table 1.

Table 1: Component parameters in the system model.

Parameter	Value	Parameter	Value
Steam turbine isentropic efficiency /%	76	cooling water pump efficiency/%	75
Steam Turbine Mechanical Efficiency/%	96	Fan Efficiency/%	80
Turbine Power Generation Efficiency/%	93	Cooling Water Pump Head/m	20
Efficiency of working fluid pump/%	70	Pinch temperature different/°C	6

2.2 CWCT-ORC Systems

For CWCT-ORC systems, we established a model (CWCT-ORC) using CWCT (Figure 4) to replace the traditional condensing equipment. The difference is that in the condensing equipment of the OCT-ORC system, heat is transferred to the ambient by the sensible heat of the cooling water, and for the CWCT-ORC system, heat is transferred to the ambient by the latent heat of the cooling water. Therefor the CWCT-ORC model needs less cooling water, leading to less energy consumption of the cooling water pump.

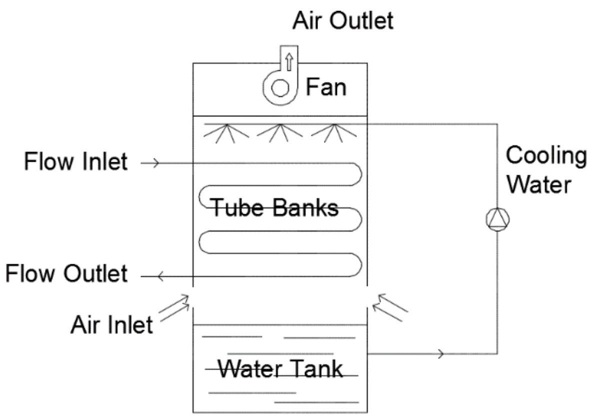

Figure 4: Schematic diagram of CWCT.

The main equations of the model are as follows:

Because the sensible heat of water is much smaller than the latent heat of gasification, it is considered in CWCT that the heat of working fluids is all carried by the latent heat of gasification of water, so the load of the cooling system is written as

$$m_{\text{orc}} \cdot (h_2 - h_4) = m_{\text{air}} \cdot \left(h_{\text{air,out}} - h_{\text{air,in}}\right) \tag{9}$$

Previous studies indicated that the effect of cooling is the best when the cooling water mass flow and air flow ratio is around 1:1. As such, the energy consumption of the cooling water pump is written as

$$m_{\text{cw}} = m_{\text{air}} \tag{10}$$

$$W_{\text{cp}} = m_{\text{cw}} \cdot g \cdot H / \left(\eta_{\text{cp}} \cdot 1000\right) \tag{11}$$

Net power of system and generation efficiency is written as

$$W = W_{\text{orc}} - W_{\text{orc,p}} - W_{\text{cw,p}} - W_{\text{fan}} \tag{12}$$

According to the typical meteorological year in Tianjin, the ambient air condition is divided into four parts: winter, summer, spring and autumn. These parts are the air inlet parameters in CWCT. In addition, a hypothesis is made in the model that the relative humidity of air reaches 100% when it leaves CWCT. Both the temperature and humidity values are the average of the seasons. The parameters are shown in Table 2.

Table 2: Air status parameters of Tianjin.

	Average temperature/°C	Average humidity/ %
Summer	24.5	75.8
Spring and autumn	12.7	58.7
Winter	-1.8	43.9

But the CWCT-ORC system has its own shortcomings. The pressure loss of CWCT in the CWCT-ORC system is greater than that in the OCT-ORC system. According to the data of cooling towers with the same refrigeration capacity provided by China Yileng Hezhong Science and Technology Co., Ltd, the pressure drop of CWCT ranges from 0.06 to 0.1 MPa. Pressure drop of CWCT is determined by its size, arrangement of heat exchanger tubes and ambient by Gan G (2001). This paper also studies the effect of different pressure losses of CWCT on the net power generation and net generation efficiency.

3 VALIDATION AND ANALYSIS OF OCT-ORC MODELS

3.1 ORC System Experiment

The ORC power generation system experimental platform is located at Huabei Oilfield. The system uses the geothermal water as the heat source, and the working fluid of the system is R245fa. The condensing equipment of the system is a shell-and-tube condenser and an open cooling tower. Until now it has completed 168 hours of continuous operation.

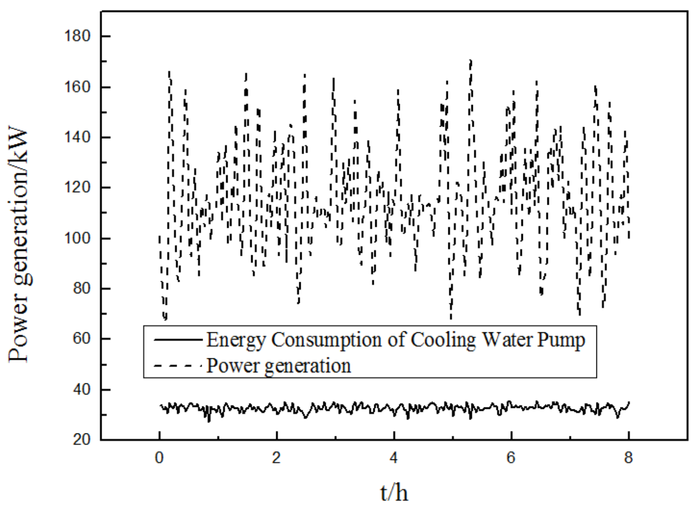

Figure 5: Comparison of cooling pump energy consumption and total power generation of the system.

Figure 5 is a comparison between the energy consumption of cooling water pump and the total power generation of the system during the experimental operation. From the figure, it can be seen that the total power generation fluctuates greatly, most of the values are between 90-140 kW, while the energy consumption of cooling water pumps is relatively stable, basically maintained between 30-40 kW. The calculation shows that the average power generation of the system in eight hours is 115 kW, while the average energy consumption of the cooling water pump is 33 kW, accounting for 28.5%.

3.2 Models and Experimental Validation

To verify the feasibility and validity of the numerical model, the model results are compared with experimental measurement. To ensure the comparability, the experiment and simulation are under the same conditions and operating parameters. In the model, the temperature of the geothermal water is set to be 110°C, the mass flow of the geothermal water is set to be 56.8 t/h, the degree of the working fluid superheat in the evaporator outlet is set to be 5°C. The results are shown in Table 3.

Table 3: Comparison of simulation and experiment results.

	Experiment	Simulation
Mass flow of R245fa/t·h-1	42.71	44.93
Temperature of evaporator inlet/°C	35.81	36.32
Temperature of evaporator outlet/°C	76.97	77
Pressure of evaporator inlet/MPa	0.676	0.643
Pressure of evaporator outlet/MPa	0.647	0.613
Temperature of condenser inlet/°C	52.59	56.28
Temperature of condenser outlet/°C	36.02	36
Pressure of condenser inlet/MPa	0.250	0.248
Pressure of condenser outlet/MPa	0.222	0.218
Temperature of cooling tower inlet/°C	26.47	20
Temperature of cooling tower outlet/°C	23.67	23
Energy consumption of cooling water pump/kW	32.88	55.69
Power generation/kW	139.15	142

In the study of the ORC system, the comparison of simulation and experiment results are shown in Table 3. The parameters of the experimental part are based on the average of 168 hours of operation in Huabei Oilfield. All of the simulation input parameters are set according to them. It can be seen from Table 3 that the simulated power generation is quite close to the measured data, with only 2.85 kW difference in case. The differences between the simulation and experimental results could be caused by the fluctuation of experimental parameters.

Table 4: Percentage of energy consumption of cooling water pump on total power generation.

	Total System Power Generation /kW	Energy Consumption of Cooling Water Pump /kW	Percentage /%
R123	420.04	69.14	16.5 %
R227ea	511.5	88.4	17.3 %
R245fa	471.42	72.12	15.3 %
R600	475.9	71.3	15.0 %
R600a	485.9	74.6	15.4 %

Table 4 shows the comparison of the system power generation of five working fluids and the energy consumption of cooling water pumps. Among them, the temperature of geothermal water is 110°C, the mass flow rate of geothermal water is 67.5 kg/s, the evaporation temperature is 80°C, and the condensation temperature is 30°C. It can be seen from the table that using R227ea as working fluid has the largest system power generation, the following are R600a, R600, R245fa and R123. But R227ea also has the largest cooling water pump energy consumption. The energy consumption of cooling water pumps with other working fluids accounts for more than 15% of the total power generation of the system. It can be seen that the excessive energy consumption of cooling water pump is a major problem of OCT-ORC system, so the following research on CWCT-ORC system is carried out in this paper.

4 COMPARISON BETWEEN OCT-ORC AND CWCT-ORC SYSTEMS

4.1 Comparison of Different Seasons of CWCT-ORC Systems

In this paper, the OCT-ORC model and the CWCT-ORC model are established and compared. For better comparison, the installed capacity is set to be 500 kW for both models, the temperature of geothermal water is set to be 105°C, the mass flow of geothermal water is set to be 243 t/h. Table 5 shows the comparison of the cooling water pump energy consumption of the two systems when the pressure loss of the CWCT is set to be 0.06 MPa. The evaporation temperature is set to be 80°C and the condensation temperature is set to be 30°C. From Table 4, it can be found that the CWCT-ORC system reduces a large proportion of the energy consumption of the cooling water pump. When using R227ea as the working fluid the CWCT-ORC system reduces the energy consumption of the cooling water pump by 61.61 kW. As for other working fluids, the CWCT-ORC system reduces the energy consumption of the cooling water pump by 49.04-52.83 kW.

Table 5: Comparison of cooling water pump energy consumption between two systems.

	OCT-ORC		CWCT-ORC	
	Energy consumption/kW	Percentage /%	Energy consumption/kW	Percentage /%
R123	65.13	13.33	16.09	3.94
R227ea	83.41	11.57	21.8	3.15
R245fa	67.69	12.39	16.88	3.43
R600	67.18	11.94	16.68	3.21
R600a	70.3	11.69	17.47	3.07

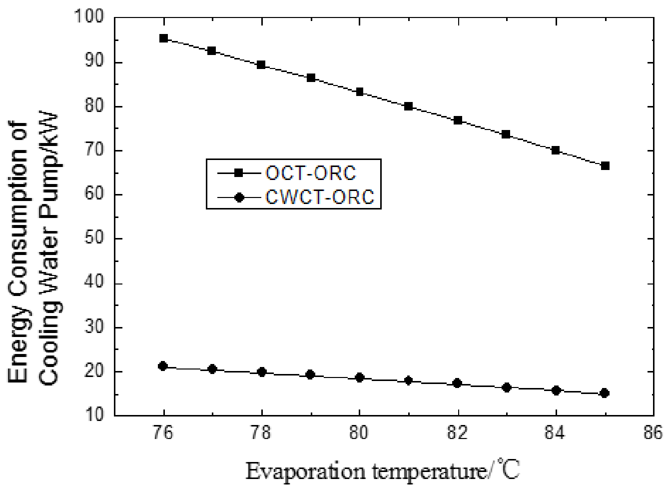

Figure 6: Effect of evaporating temperature on energy consumption of two system cooling water pumps when using R123.

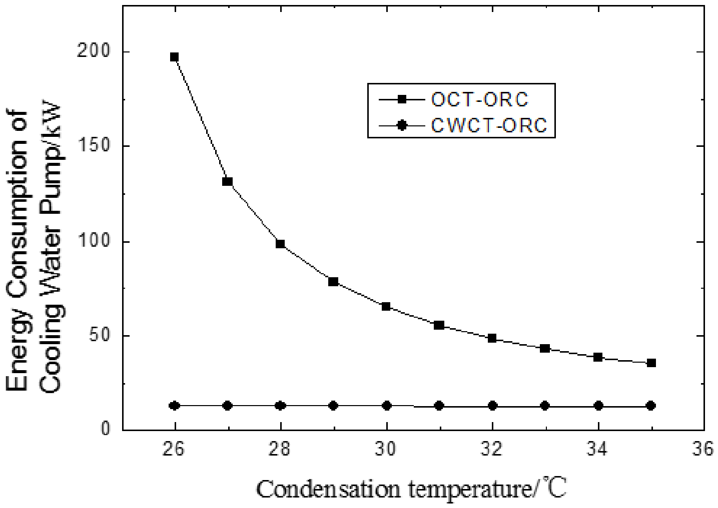

Figure 7: Effect of condensation temperature on energy consumption of two system cooling water pumps when using R123.

Figure 6 and Figure 7 show the effect of evaporation and condensation temperature on energy consumption of cooling water pumps in two systems. Among them, the temperature of heat source is 105°C, the mass flow rate of heat source is 67.5 kg/s, the pressure drop of heat exchanger in OCT-ORC system is 0.03 MPa, the pressure drop of evaporator in CWCT-ORC system is 0.03 MPa, and the pressure drop of CWCT is 0.06 MPa. In Figure 6, the variation range of evaporation temperature is 76-85°C, the condensing temperature is 30°C, and in Figure 7, the evaporation temperature is 80°C, the variation range of condensing temperature is 30°C. It can be seen from Figure 6 and Figure 7 that evaporation temperature and condensation temperature have much greater influence on OCT-ORC system than CWCT-ORC system. This is because the sensible heat of water is about 4.2 kJ/kg·K and the latent heat of vaporization is 2453.9 kJ/kg when the temperature of cooling water is 20°C, but the latent heat of vaporization of working substance is above 100 kJ/kg. It is still very large for the sensible heat of water, but the latent heat of water is much larger than that. So evaporation and condensation temperature have great influence on OCT-ORC system.

Table 6 shows the difference between the net power generation and net generation efficiency of two systems. Evaporation temperature is set to be 80°C, condensation temperature is set to be 30°C. The CWCT pressure loss is set to be 0.06 MPa. As it can be seen from Table 6, when using R227ea as the working fluid, the CWCT-ORC system has the greatest net power generation, when using R600 as the working fluid, the CWCT-ORC system has the greatest net generation efficiency.

Table 6 Comparison of CWCT on the performance of CWCT-ORC systems

	Ney power generation/kW			Net generation efficiency/%		
	OCT-ORC	CWCT-ORC	Difference value	OCT-ORC	CWCT-ORC	Difference value
R123	368	335.5	-32.5	4.71	4.714	0.004
R227ea	419.6	449.30	29.7	4.19	4.628	0.438
R245fa	406.1	400	-6.1	5.11	5.315	0.205
R600	404.3	410.2	5.9	5.22	5.493	0.273
R600a	406.6	423.5	16.9	5.06	5.409	0.349

From Table 6 we can see that using CWCT as the condensing equipment leads to a significant improvement on both the net power generation and net generation efficiency when using R227ea and R600a. When the installed capacity of the system is 500 kW and using R227ea as working fluid, compared to the OCT-ORC system, the CWCT-ORC system has the most significant improvement of the net power generation and net generation efficiency, with its net power generation increased by 29.4 kW, net power generation efficiency increased by 0.44%. Using R600 and R600a as working fluids, the net power generation of the CWCT-ORC system increases 5.9 kW and 16.9 kW, the net generation efficiency increases 0.27% and 0.35%, respectively, when using R123 and R245fa as working fluids, the net power generation and net generation efficiency of the CWCT-ORC system exhibits a little decrease, indicating that they are unsuitable for CWCT-ORC systems.

4.2 Effect of Pressure Loss on CWCT-ORC System

Pressure loss of the CWCT is within the range of 0.06-0.1 MPa for the 500kW power generation systems according to its size, the arrangement of heat exchanger tubes and ambient conditions. For studying the effect of the CWCT pressure loss on the system performance, the pressure loss of the CWCT is set to be 0.06 MPa, 0.08 MPa and 0.1 MPa.

Table 7: Effect of pressure loss of CWCT on the performance of CWCT-ORC systems.

	Ney power generation/kW			Net generation efficiency/%		
CWCT pressure loss	0.06MPa	0.08MPa	0.1MPa	0.06MPa	0.08MPa	0.1MPa
R123	335.5	290.2	249.2	4.714	4.077	3.502
R227ea	449.30	427.5	406.5	4.628	4.404	4.188
R245fa	400	365.8	334	5.315	4.859	4.438
R600	410.2	381.9	355.2	5.493	5.115	4.757
R600a	423.5	400	377.4	5.409	5.109	4.821

Table 7 shows the comparison of the net power generation and net generation efficiency of the CWCT-ORC system. From the data in Table 7, it is indicated that the net power generation and net generation efficiency decrease quickly with the increase of the pressure loss. So R227ea can be used as the working fluid of the CWCT-ORC system when the pressure drop of CWCT is in the range of 0.06-0.088 MPa, for R600 is in the range of 0.06-0.064 MPa, for R600a is in the range of 0.06-0.075 MPa, respectively. The reason is, although CWCT reduces the energy consumption of cooling water pump, the increase of pressure drop leads to the decrease of total power generation. Therefore, when the pressure drop increases to a certain value, the net power generation of CWCT-ORC system will be less than that of OCT-ORC system.

Under the condition of controlling the CWCT pressure loss, the CWCT can be used to replace the traditional condensing equipment when using R227ea, R600, R600a. The pressure loss of the CWCT has a great effect on the system net power generation and net generation efficiency. Therefore, it is necessary to study the pressure drop of CWCT in the future.

5 CONCLUSION

This paper presents two models of ORC power generation system driven by geothermal water. By comparing OCT-ORC and CWCT-ORC systems, the following conclusions are drawn:

(1) For OCT-ORC and CWCT-ORC systems, using R227ea as working fluid has the largest system power generation, the following are R600a, R600, R245fa and R123;

(2) Evaporation temperature and condensation temperature have much greater influence on OCT-ORC system than CWCT-ORC system, and the influence of condensation temperature is greater;

(3) CWCT-ORC systems effectively reduce the energy consumption of the cooling water pump. When using R227ea as the working fluid, the CWCT-ORC system has the greatest reduction of energy consumption for the cooling water pump.

(4) Pressure loss of the CWCT has great effect on the net power generation and net generation efficiency. With the increase of the pressure loss of the CWCT from 0.06 to 0.1 MPa, the net power generation and net generation efficiency of the CWCT-ORC system decrease quickly. In addition, different working fluids are suitable for different pressure loss. So how to design the cooling tower to decrease the pressure drop is the key work. The future research emphasis will be focused on it.

ACKNOWLEDGEMENTS

This work was supported by the National Key Research and Development Program of the 13th Five-Year Plan of China (No. 2018YFB1501805).

REFERENCE

Boydak, Özlem, Ekmekçi, İsmail, Yilmaz M , et al. Thermodynamic investigation of organic Rankine cycle (ORC) energy recovery system and recent studies[J]. Thermal Science, 2018, 22(1).

Alkhedhair A, Gurgenci H, et al. Numerical simulation of water spray for pre-cooling of inlet air in natural draft dry cooling towers[J]. Applied Thermal Engineering, 2013, 61(2):416-424.

Yang L J, Du X Z, et al. Wind effect on the thermo-flow performances and its decay characteristics for air-cooled condensers in a power plant[J]. International Journal of Thermal Sciences, 2012, 53(3):175-187.

Yang L J, Chen L, et al. Effects of ambient winds on the thermo-flow performances of indirect dry cooling system in a power plant[J]. International Journal of Thermal Sciences, 2013, 64(2):178–187.

Hooman K. Dry cooling towers as condensers for geothermal power plants[J]. International Communications in Heat & Mass Transfer, 2010, 37(9):1215-1220.

Preez A F D, Kröger D G. Effect of wind on performance of a dry-cooling tower[J]. Heat Recovery Systems & Chp, 1993, 13(2):139-146.

Preez A F D, Kröger D G. The effect of the heat exchanger arrangement and wind-break walls on the performance of natural draft dry-cooling towers subjected to cross-winds[J]. Journal of Wind Engineering & Industrial Aerodynamics, 1995, 58(3):293-303.

Al-Waked R, Behnia M. The performance of natural draft dry cooling towers under crosswind: CFD study[J]. International Journal of Energy Research, 2004, 28(2):147–161.

Jiang J J, Liu X H, et al. Experimental and numerical analysis of a cross-flow closed wet cooling tower[J]. Applied Thermal Engineering, 2013, 61(2):678-689.

Kloppers J C, Kröger D G. The Lewis factor and its influence on the performance prediction of wet-cooling towers[J]. International Journal of Thermal Sciences, 2005, 44(9):879-884.

Heidarinejad G, Karami M, et al. Numerical simulation of counter-flow wet-cooling towers. Int J Refrig[J]. International Journal of Refrigeration, 2009, 32(5):996-1002.

Papaefthimiou V D, Rogdakis E D, et al. Thermodynamic study of the effects of ambient air conditions on the thermal performance characteristics of a closed wet cooling tower[J]. Applied Thermal Engineering, 2011, 33-34(1):199-207.

Saravanan M, Saravanan R, et al. Energy and exergy analysis of counter flow wet cooling towers[J]. Thermal Science, 2008, 12(2):69-78.

Hajidavalloo E, Shakeri R, et al. Thermal performance of cross flow cooling towers in variable wet bulb temperature[J]. Energy Conversion & Management, 2010, 51(6):1298-1303.

Wang L, Li N. Exergy transfer and parametric study of counter flow wet cooling towers[J]. Applied Thermal Engineering, 2011, 31(5):954-960.

Wang L, Li N. Exergy transfer and parametric study of counter flow wet cooling towers[J]. Applied Thermal Engineering, 2011, 31(5):954-960.

Thirapong, M, Wanchai A, et al. An Exergy Analysis on the Performance of a Counterflow Wet Cooling Tower. Applied Thermal Engineering, 27 (2007), 5-6, pp. 910-917

Rubio-Castro E, Serna-González M, et al. Optimization of mechanical draft counter flow wet-cooling towers using a rigorous model[J]. Applied Thermal Engineering, 2011, 31(16):3615-3628.

Khan J U R, Zubair S M. A study of fouling and its effects on the performance of counter flow wet cooling towers[J]. ARCHIVE Proceedings of the Institution of Mechanical Engineers Part E Journal of Process Mechanical Engineering 1989-1996 (vols, 2004, 218(218):43-51.

Saidi M H, Sajadi B, et al. Energy consumption criteria and labeling program of wet cooling towers in Iran[J]. Energy & Buildings, 2011, 43(10):2712-2717.

Gan G, Riffat S B, et al. Application of CFD to closed-wet cooling towers[J]. Applied Thermal Engineering, 2001, 21(21):79-92.

Walraven D, Laenen B, et al. Minimizing the levelized cost of electricity production from low-temperature geothermal heat sources with ORCs: Water or air cooled? [J]. Applied Energy, 2015, 142:144-153.

Nomenclature

c	sensible heat of water, [kJkg^{-1}K^{-1}]	λ	thermal conductivity, [kWm^{-1}k^{-1}]
d	pipe diameter, [mm]	μ	Viscosity, [kgm^{-1}s^{-1}]
f	friction coefficient	**Subscripts**	
g	gravity of acceleration, [ms^{-2}]	air	air
G	mass velocity, [kgm^{-1}s^{-1}]	cw	cooling water
h	enthalpy, [kJkg^{-1}]	e	generation
H	lift, [m]	fan	fan
l	Length, [mm]	hw	hot water

m	mass flow rate, [kgs^{-1}]	in	inlet
n	tube row number	is	isentropic
Q	heat exchange, [kW]	m	mechanical
Q_{air}	volume flow of air, [m^3s^{-1}]	net	net
T	temperature, [K]	orc	organic Rankine cycle
W	power, [kW]	out	outlet
	Greek symbols	output	output
η	efficiency, [%]	p	pump
ρ	density, [kgm^{-3}]		